Distances between Tropomyosin Sites Across the Muscle Thin Filament Using Luminescence Resonance Energy Transfer: Evidence for Tropomyosin Flexibility

Yaodong Chen and Sherwin S. Lehrer*

Muscle and Motility Group, 64 Grove Street, Boston Biomedical Research Institute, Watertown, Massachusetts 02472

Received April 22, 2004; Revised Manuscript Received June 17, 2004

ABSTRACT: To obtain information about the interaction of tropomyosin (Tm) with actin associated with the regulatory states of the muscle thin filament, we used luminescence resonance energy transfer (LRET) between Tb^{3+} as a donor and rhodamine as an acceptor. A novel Tb^{3+} chelator, *S*-(2-nitro-5-thiobenzoate)-cysteaminyl-DTPA-Cs124, was synthesized, which specifically labels Cys groups in proteins. With the Tb chelate as the donor and tetramethylrhodamine-5-maleimide as the acceptor, both bound to specific Cys groups of Tm, we obtained 67 Å as the distance between Tm's across the actin filament, a much shorter value than that obtained from structural studies (72−86 Å). The difference appears to be due to submillisecond motion associated with Tm flexibility, which brings the probes closer during the millisecond lifetime of the donor. Ca^{2+} did not change the energy transfer with the reconstituted thin filament, but myosin subfragment 1 decreased the transfer, consistent with either a 5−6 Å increase in distance or, more likely, a decrease in flexibility.

Tropomyosin (Tm),[1] a component of the native actin thin filament, acts with troponin (Tn) and Ca^{2+} to regulate muscle contraction (See reviews of refs *1* and *2*). An extension of the original steric blocking model of thin-filament regulation (*3*−*5*) was proposed by McKillop and Geeves (*6*) involving three biochemical states of the thin filament, blocked, closed, and open, which affect myosin binding. In the absence of Ca^{2+}, the blocked state is mostly occupied, which causes the inhibition of the initial or weak binding of myosin heads. Ca^{2+} causes a shift to the closed state, which allows low-affinity myosin binding, but Tm mostly blocks the strong binding and activation of ATPase associated with force generation. When Tm moves to the open state because of the cooperative binding of myosin heads, the thin filament is activated.

Structural studies have indicated that Tm moves to a different position on the actin−Tm−Tn thin filament induced by Ca^{2+} with further movement associated with myosin binding, allowing for an apparent relationship between the three positions of Tm and the three biochemical states (*7*−*11*). Although these EM image reconstruction methods obtained evidence for three positions of Tm on actin in the actin−Tm−Tn thin filament, it has been difficult to obtain solution evidence for Tm movement. Several FRET (Förster or fluorescence-detected resonance energy transfer) studies, which measured the distance changes between Tm and F actin, obtained different results. Some measurements did not show a distance change between Tm and actin induced either by Ca^{2+} or myosin binding (*12*, *13*), although a significant distance change between troponin and actin can be observed (*13*−*16*). A more recent FRET study using frequency domain lifetime detection methods indicated that Ca^{2+} mainly affects the distance between one of the two chains of Tm to F actin, consistent with Tm rolling over the F-actin surface (*17*). Graceffa observed that the distance between smooth-muscle Tm and F-actin changes, induced by myosin subfragment 1 (S1) and heavy meromyosin (*18*, *19*). Recent lifetime measurements indicated that the S1-induced movement was consistent with a rolling of Tm over the actin surface (*20*).

To obtain further information on Tm movement, the energy-transfer technique of LRET (luminescence resonance energy transfer) was employed with the use of a thio-reactive Tb^{3+} chelate as the donor. Lanthanide chelates have desirable donor properties (*21*−*27*): millisecond lifetimes, narrow and multiple emission bands, unpolarized emission, and large Stokes shift. These characteristics enable temporal and spectral discrimination against background fluorescence, leading to high-detection sensitivities. In addition, with appropriate acceptor labels, such as rhodamine, large distances can be measured with LRET (∼50−80 Å) because of the large Förster critical transfer distance $R_0 = 57$ Å. These distances are in the range expected between equivalent sites on Tm across actin, and therefore changes in distances associated with thin-filament regulation may be monitored.

We synthesized a novel lanthanide chelate, *S*-(2-nitro-5-thiobenzoate)cysteaminyl-DTPA-Cs124 (NbS·SCy-DTPA-Cs124), based on syntheses of similar compounds (*21*, *28*, *29*). The label consists of three functional groups: A DTPA group, which binds Tb^{3+}; a NbS group, which can specifically react with Cys groups; and an antenna group (Cs124), which efficiently transfers the absorbed energy to Tb^{3+}. The

† This work was supported by NIH Grants HL 22461 and AR 41637.

* To whom correspondence should be addressed. E-mail: lehrer@bbri.org. Telephone: 617-658-7812. Fax: 617-972-1753.

‡ Present address: Department of Cell Biology, Duke University Medical Center, Durham, NC, 27710. E-mail: y.chen@cellbio.duke.edu.

[1] Abbreviations: S1, myosin subfragment 1; Tm, tropomyosin; Tn, troponin; (NbS·SNb), 5,5′-dithiobis(2-nitrobenzoate); LRET, luminescence-detected resonance energy transfer.

10.1021/bi049186v CCC: $27.50
Published on Web 08/19/2004

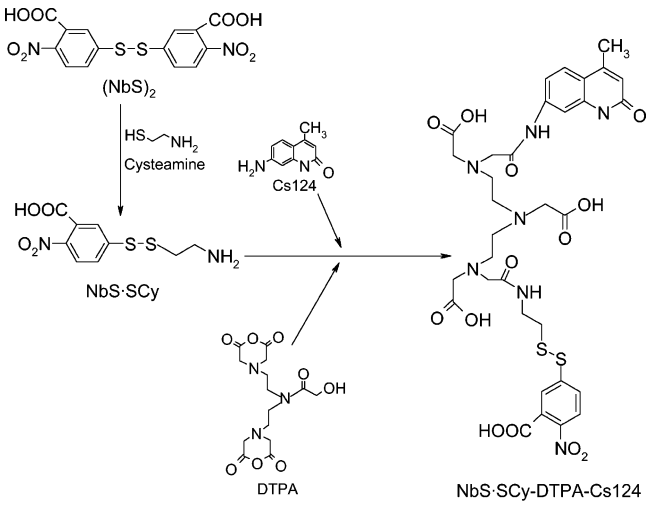

FIGURE 1: Scheme of the synthesis of NbS·SCy-DTPA-Cs124. (See the Materials and Methods for details).

Cs124 thereby eliminates the requirement for inefficient direct excitation of the weakly absorbing Tb^{3+}. With the Tb chelate bound to Tm as the donor and tetramethylrhodamine-5-maleimide on Tm as the acceptor, we obtained 67 Å as the apparent distance between Tm's bound to actin. This is shorter than 73−76 Å, the distance calculated from structural data (*30*−*33*), suggesting submillisecond relative motion, which allows a greater degree of transfer at a closer distance during the millisecond lifetime of the donors. The observation of significant LRET from a large fraction of Tm's that bind to opposite strands of the actin filament indicates that they are in-register. However, a significant fraction did not transfer, suggesting that some Tm random binding to actin occurs. Ca^{2+} produced little or no change in the distance between Tm's across the actin−Tm−Tn filament. However, binding of myosin S1 to actin−Tm or actin−Tm−Tn produced a decrease in energy transfer between Tm's consistent with either a ∼5−6 Å increase in distance or a decrease in flexibility between the two Tm's.

MATERIALS AND METHODS

Chemicals. The following chemicals and their sources were used in the synthesis of the probe and for protein labeling: 5,5′-dithiobis(2-nitrobenzoate) (NbS·SNb) from Sigma; diethylenetriamine-pentaacetic dianhydride (DTPA dianhydride), 2-aminoethanethiol hydrochloride (cysteamine), carbostyril 124 (Cs124), dimethyl sulfoxide anhydride (DMSO) from Aldrich; and tetramethylrhodamine-5-maleimide (TMR-5-mal) from Molecular Probes.

Synthesis of NbS·SCy-DTPA-Cs124. NbS·SCy-DTPA-Cs124 was synthesized using NbS·SNb, cysteamine hydrochloride, DTPA dianhydride, and Cs124 by modifying the methods of Bertrand et al. (*28*) and Chen and Selvin (*21*) (Figure 1). Cysteamine hydrochloride (22 mM) in 500 mM CHES buffer (pH 8.6) was reacted with 20 mM NbS·SNb dissolved in DMSO for $^1/_2$ h at room temperature. The absorption at 412 nm because of the liberated NbS anion was monitored to make sure that the reaction was complete. Cs124 (8.7 mg) dissolved in DMSO was then mixed into the solution to a final concentration of 20 mM and stirred for 10 min. DPTA dianhydride (21.4 mg), dissolved in anhydrous DMSO by heating to 70∼80 °C, was added immediately into the solution with strong stirring to a final concentration of 23 mM. The solution was allowed to react overnight. The final solution was spun to remove some insoluble precipitates. NbS·SCy-DTPA-Cs124 was isolated by reverse-phase HPLC as follows: the solution was loaded on a Vydac C-8 208TP510 column and eluted for 40 min with a 20−50% acetonitrile/H_2O gradient containing 0.1% trifluoroacetic acid at a flow rate of 1 mL/min and detected at 330 and 375 nm. The NbS·SCy-DTPA-Cs124 eluted at 35% acetonitrile. MALDI mass spectra data showed that the molecular weight of this component was 805.8 (the calculated molecular weight is 804). The steps of synthesis are shown in Figure 1.

Labeling of Proteins. We used ααTm from chicken skeletal muscle purified by standard methods and 2 different recombinant single Cys mutants of α gizzard smooth-muscle Tm (GTm), [S56C/C190S (Tm56) and D100C/C190S (Tm100)] (*34*). The terbium-labeled chelate was simply prepared by mixing 2 mM NbS·SCy-DTPA-Cs124 in 20 mM Hepes buffer (pH 7.5) with $TbCl_3$ (0.9 Tb/probe molar ratio) for 20 min. Then, a 10-fold molar ratio of NbS·SCy-(Tb^{3+}-DTPA)-Cs124 to Tm (∼10−30 μM) was reacted in 20 mM Hepes, 5 M guanidine hydrochoride (GuHCl), 50 mM NaCl, and 5 mM $MgCl_2$ (pH 7.5), for 2 h at room temperature. The absorption at 412 nm from the released NbS^- group increased, indicating an efficient reaction of the probe with Cys. The sample was then dialyzed versus GuHCl buffer (20 mM Hepes and 5 M GuHCl at pH 7.5), high-salt buffer (20 mM Hepes, 500 mM NaCl, and 5 mM $MgCl_2$ at pH 7.5), and finally 20 mM Hepes, 50 mM NaCl, and 5 mM $MgCl_2$ at pH 7.5 separately to renature Tm. The label/Tm ratio varied between ∼40−60%. Actin and myosin subfragment 1 was from rabbit skeletal muscle purified by standard methods (*52*).

Another Tm sample was labeled with the acceptor by reacting a 10-fold molar excess of TMR-5-maleimide with ∼10−30 μM Tm in GuHCl buffer, dialyzing successively versus GuHCl buffer, high-salt buffer, and final buffer as indicated above.

The acceptor/Tm label ratio was near 2 in agreement with one Cys on each chain of the dimer. The absorption spectrum of TMR consists of a peak at 550 nm and a shoulder at 520 nm. However, some rhodamine-labeled proteins have a changed absorption spectrum consisting of an increase in the 520-nm contribution because of rhodamine−rhodamine dimerization of locally proximal probes (*35*, *36*). The observation of a large contribution at 520 nm because of the absorption of TMR−Tm (A_{520}/A_{550}) = 0.9, indicates close proximity of rhodamines attached to equivalent Cys groups of the in-register coiled-coil chains. This result is analogous to the pyrene−pyrene interaction from labels at the same Cys, which resulted in excimer fluorescence (*52*). Some samples, however, had an absorption spectrum with a much greater 520:550 nm ratio, suggesting the presence of an aggregated excess label. In these cases, aggregation was verified when we obtained a normal absorption spectrum after denaturing with 0.1% SDS or 6 M GuHCl and dialyzing into final buffer to remove the excess label and to renature the sample.

To measure the interchain distance between positions 56 and 100 in ααGTm, donor-labeled Tm56 was mixed with 5-fold excess acceptor-labeled Tm100 ($Tm56^D$ and $Tm100^A$)

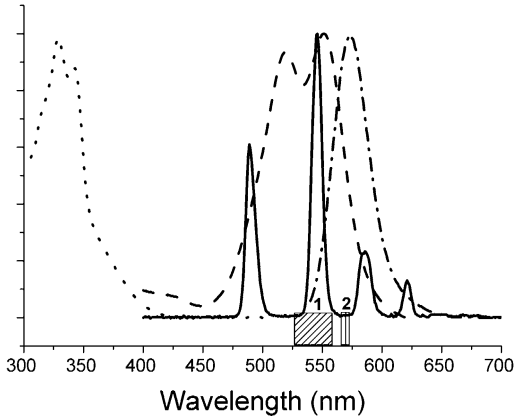

FIGURE 2: Donor absorption (···) and luminescence (—) and acceptor (TMR) absorption (- - -) and fluorescence (-·-). All spectra are normalized at peak intensity. Note the overlap of emission of Tb^{3+} with the absorption of rhodamine. Labels 1 and 2 show the band pass of filters that we used (filter 1 = 545 ± 5 nm, and filter 2 = 568 ± 2 nm).

in 5 M GuHCl buffer and dialyzed versus high-salt buffer and then final buffer to renature. The excess acceptor-labeled chains ensured that molecules containing donors were mainly present as $Tm56^{D}-Tm100^{A}$ heterodimers.

For measuring the distance between Tm sites across F actin, 0.2 μM skeletal ααTm labeled with NbS·SCy(Tb^{3+}-DTPA)-Cs124 as the donor (Tm^{D}) and 0.8 μM skeletal ααTm labeled with TMR-5-maleimide as the acceptor (Tm^{A}) was mixed together in a 20 mM Hepes, 50 mM NaCl, and 5 mM $MgCl_2$ (pH 7.6) solution and added to 10 μM F actin, with an incubation for $^1/_2$ h at room temperature. Effects of myosin S1 and Tn ± Ca^{2+} were determined by adding 5 μM S1 and 1 μM Tn, respectively, in the presence (0.1 mM $CaCl_2$) or absence of Ca^{2+} (1 mM EGTA).

Measurement of Luminescence Decay. Time-resolved spectra were measured with an instrument constructed by Aviv Corp. (Lakewood, NJ), which coupled a VSL-337ND-S nitrogen laser (337 nm, LSI Corp.) to an AVIV filter fluorometer (Model ATFF-212). The computer-controlled filter fluorometer triggers the pulsed laser, and data collection is initiated by the laser pulse. The luminescence was collected through either a 545 ± 5 nm filter or 568 ± 2 nm filter (Omega). The 545 ± 5 nm filter was used to detect the direct Tb^{3+} luminescence, whereas the 568 ± 2 nm filter, which monitors the signal in the rhodamine spectrum, was used to detect the Tb^{3+} luminescence transferred to the rhodamine (Figure 2). The temperature of the measurement was 25 °C, controlled thermostatically with the Peltier device in the instrument.

The emission of the donor [NbS·SCy(Tb^{3+}-DTPA)-Cs124] was obtained at 545 nm, where there is no contribution from the rhodamine emission. The emission at 568 nm only originates from rhodamine because there is no contribution from Tb^{3+} at that wavelength. However, at 568 nm, the large amount of directly excited rhodamine fluorescence present in the nanosecond time region is gated out by the instrument so that only the transferred Tb^{3+} emission is observed. Donor-only Tm decays detected at 545 nm were fitted with up to 2 lifetimes. In the absence of the acceptor, a small lifetime contribution of about ~0.3−0.4 ms and a large contribution of about 1.4 ms is observed. In the presence of the acceptor, 3 lifetimes were needed to fit the decays at 545 and 568 nm. The longest decay component at 568 nm directly gives the lifetime because of transfer, τ_{DA}. The data were fit using Origin software.

Theory (17, 37). According to the Förster theory, the rate of energy transfer from a donor to an acceptor (k_T) is

$$k_T = \frac{1}{\tau_D}\left(\frac{R_0}{r}\right)^6 \quad (1)$$

where τ_D is the decay time of the donor in the absence of the acceptor, R_0 is the Förster distance, and r is the donor−acceptor distance.

The reduced lifetime in the presence of acceptor, τ_{DA} is

$$\frac{1}{\tau_{DA}} = \frac{1}{\tau_D} + k_T \quad (2)$$

The energy transfer efficiency is given by the reduction in lifetime

$$\boldsymbol{E} = 1 - \tau_{DA}/\tau_D \quad (3)$$

and the distance r is

$$r = R_0\left(\frac{1}{E} - 1\right)^{1/6} \quad (4)$$

where R_0 is the critical transfer distance, defined below. The rate of energy transfer (k_T) is

$$k_T = \frac{1}{\tau_D}\sum_i\left(\frac{R_0}{r_i}\right)^6 \quad (5)$$

For a multi-D−A system, the apparent distance r_a can be defined by ref *17* with

$$r_a = \left(\sum_{i=1}^{N}\frac{1}{r_i^6}\right)^{-1/6} \quad (6)$$

This apparent distance represents the D−A distance "seen" by our LRET experiment. R_0 is defined by the equation

$$R_0^6 = (8.79 \times 10^{-5})n^{-4}\kappa^2 Q_0 J \quad (7)$$

where n is the refractive index of the medium, taken as 1.33 (*19*, *32*); κ^2 is the orientation factor, taken as $^2/_3$; Q_0 is the quantum yield of the donor in the absence of the acceptor, taken as 0.468, the value in water (*38*); and J is the spectral overlap integral (in M^{-1} cm^{-1} nm^4) between the donor emission $F_d(\lambda)$ and acceptor absorption $\epsilon_A(\lambda)$ spectrum, defined by

$$J = \int F_d(\lambda)\,\epsilon_A(\lambda)\lambda^4\,d\lambda / \int F_d(\lambda)\,d\lambda \quad (8)$$

We obtained a value for R_0 of 57 Å.

RESULTS

Properties of NbS·SCy-DTPA-Cs124. The labeling reagent contains the aromatic disulfide moiety, 2-nitro-5-dithiobenzoate, NbS, which is released as the anion during the labeling reaction, allowing the kinetics to be monitored using its absorption at 412 nm (*29*). The Figure 3 insert illustrates the reaction kinetics between the probe and rabbit skeletal

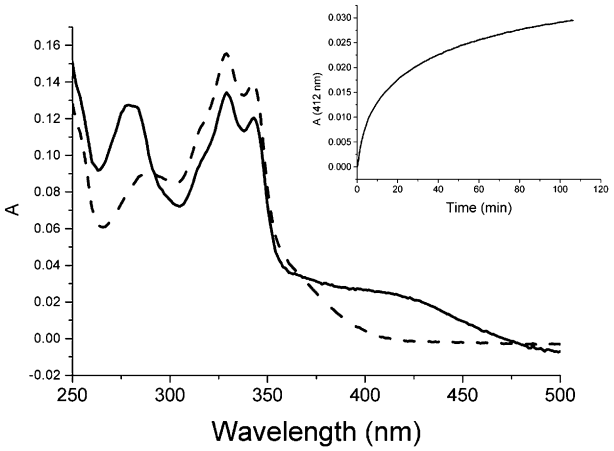

FIGURE 3: Absorption spectra of NbS·SCy-DTPA-Cs124 before (- - -) and after (—) the reaction with Tm. Tm (2 μM) in 50 mM CHES buffer (pH 8.6) was reacted with 10 μM NTBC-DTPA-Cs124 at 35 °C. The insert shows the reaction rate of NbS·SCy-DTPA-Cs124 with rabbit skeletal Tm monitored by the absorption of the liberated NbS ion.

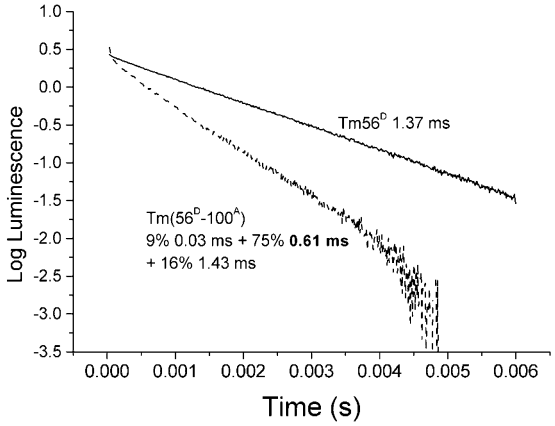

FIGURE 4: Intramolecular LRET between positions 56 and 100 on different chains of the Tm dimer. Luminescence decay of the Tb^{3+} donor at Cys 56 ($Tm56^D$) in the absence (—) and presence of the TMR (- - -) acceptor at Cys 100 ($Tm100^A$) within the Tm heterodimer. The decay was detected at 545 nm.

Tm. Rabbit skeletal Tm is a dimer of two chains, α and β, in a 60:40 mixture of αα and αβ, respectively, with the α and β chains containing 1 and 2 Cys, respectively, [Cys/Tm = 2.4 (*39*)]. From the final change in absorption at 412 nm (Figure 3), a labeling ratio of 1.5 probe/Tm was estimated. Thus, about 62% of the available Cys was labeled. The labeling reagent, NbS·SCy-DTPA-Cs124, has a characteristic absorption spectrum, with two peaks, 325 and 345 nm, because of Cs124, as well as a shoulder from 350 to 400 nm because of a contribution from the NbS group whose absorption peak at 325 nm overlaps the Cs124 absorption. The reaction of rabbit skeletal Tm with the label produced changes in the spectrum: a contribution from the protein at 280 nm, a decrease at 325 nm because of loss of NbS, and an increase at 412 nm because of the liberated NbS ion (Figure 3).

Energy Transfer between Position 56 and 100 in ααGTm. Energy-transfer measurements were made within gizzard-muscle ααTm using a recombinant mutant heterodimer containing the Tb^{3+} donor at Cys 56 on one mutant chain and a rhodamine acceptor at Cys 100 on the other mutant chain (see the Materials and Methods). This allowed a comparison of the experimentally determined distance with the known distance between α carbons of equivalent residues of a coiled-coil Tm.

Figure 4 shows the donor-alone and donor—acceptor decay curves. A single-exponential decay with a lifetime of 1.37 ms fit the donor-alone data. In the presence of the acceptor, a three-component fit was required. The 1.43-ms component, with a lifetime close to the donor-alone value is the contribution of donor-labeled molecules, which do not "see" the acceptors. This is due to the presence of homodimer Tm^D56—Tm^D56 molecules. About 78% of the luminescence has a shortened lifetime of 0.61 ms because of energy transfer. The observed 30 μs component is probably due to photomultiplier ringing caused by rhodamine fluorescence present at 545 nm. The ringing is a greater problem at 568 nm, where rhodamine fluorescence is very intense. From the reduction in the donor lifetime from 1.37 to 0.61 ms, it is calculated that the energy-transfer efficiency is 56.2% and that the distance between the donor and acceptor is therefore 55 Å (see the Theory). A separate Gaussian distance distribution fit of the data gave a distance of 56 Å with a distribution width, σ, of 5 Å.

Measurements of millisecond decay at 568 nm, which should only give the Tb^{3+} luminescence transferred to rhodamine, shows short lifetime components because of photomultiplier ringing caused by the intense rhodamine fluorescence, which is not completely gated out (*40*). Because this ringing does not die out until 0.1—0.2 ms, only the longest lifetime component was used. This value was 0.6 ms, the same as the transferred value obtained at 545 nm.

The Tm—Tm distance can be compared to a comparable distance obtained from an X-ray structure of tropomyosin (*41*). Positions from the X-ray structure were chosen to be 44 residues apart and in the same positions of the 7 residue repeat (Tm14D and Tm58D), respectively. From the model, the distance between α carbons at equivalent residues at 44 residues apart is about 65 Å (Figure 5A). The 15% smaller value obtained by LRET is probably due to the flexibility of the probe-containing domain of Tm in the submillisecond time regime, which on the millisecond lifetime of the donor can result in a greater transfer than a static molecule (*25*). When this hetero-labeled Tm was bound to actin, the energy transfer decreased from 56 to 51%, reflecting either an average increase in distance from 55 to 57 Å or a reduction in the flexibility expected in the complex (*42*, *43*).

Distance between Tm Sites across F Actin. The actin—Tm filament was reconstituted by mixing excess F actin with a solution containing chicken skeletal ααTm with 4 times as much acceptor-labeled (Tm^A, 0.8 μM) as donor-labeled Tm (Tm^D, 0.2 μM). This increased the probability for a high degree of energy transfer between Tm molecules bound to actin on opposite sides of the filament.

In Figure 6, we show the luminescence decay of the donor-labeled sample bound to unlabeled actin in the absence and presence of acceptor-labeled actin. The decays fit well to a long lifetime of 1.44 ms (contribution 0.90) and a short lifetime at 0.41 ms (contribution 0.10). The Tb^{3+} luminescence decays of donor—acceptor samples were detected both at 545 nm (direct Tb^{3+} detection) and 568 nm (acceptor-sensitized Tb^{3+} transfer). At 545 nm, the decay was fit to three components (Figure 6 and Table 1): (1) an appreciable contribution from a component of 1.44 ms because of Tb^{3+}

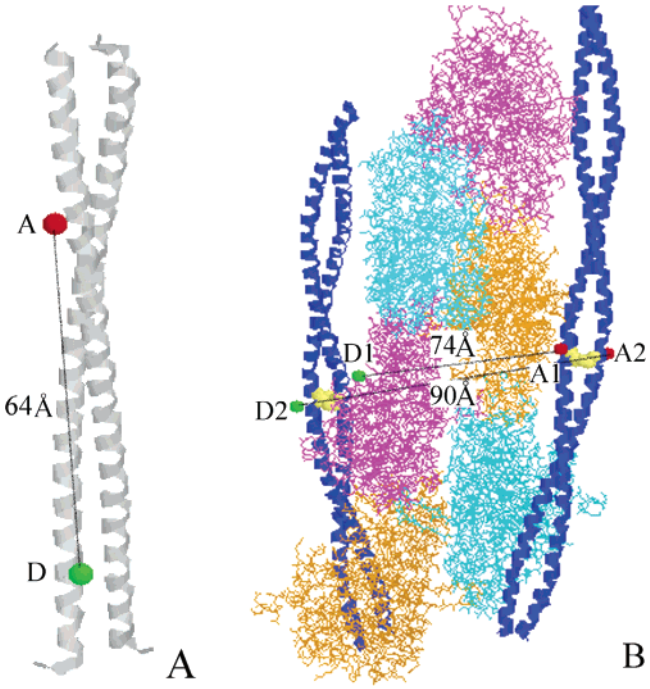

FIGURE 5: (A) Atomic model of a region of the Tm coiled-coil structure from Brown et al. (*41*). Positions from the X-ray structure were chosen to be 44-residues apart, $Tm14^D$ and $Tm58^D$, in the same position of the 7-residue repeat with Tm56 and Tm100. They are indicated by green and red balls, respectively, having about the same dimensions as the probes. From the model, the distance between α carbons at equivalent residues at 44-residues apart is 64.3−65.8 Å. (B) Atomic model of the Tm−F-actin complex from Lorenz et al. (*30*). D1 and D2 (green dots) show the approximate position of the Tb^{3+} chelates labeled with Tm. A1 and A2 (red dots) show the approximate position of the rhodamine probes. The shortest and longest distances between the donors and acceptors are indicated.

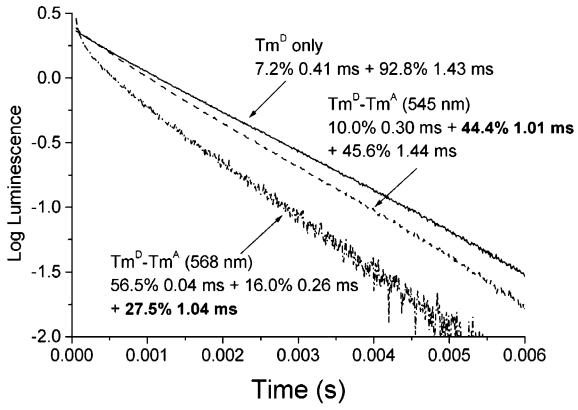

FIGURE 6: Comparison of the decays detected at 545 and 568 nm between Tb^{3+} at Cys 190 of Tm (Tm^D) and TMR at Cys 190 of Tm (Tm^A) across the actin filament.

luminescence, which is not transferred; (2) a component of 1.04 ms because of energy transfer; and (3) a component of 0.3 ms because of the ringing of the photomultiplier. The 568-nm decay was best fit to three components in which the major component, 1.04 ms, is due to energy transfer and two shorter components most likely arising from photomultiplier ringing because of intense rhodamine fluorescence, which could not be completely gated out. From eqs 3 and 4, it is calculated that the energy-transfer efficiency is 27.8%, and therefore the apparent distance between Tm's is 67 Å (Table 1). This is shorter than the average apparent distance, r_a, between probes (73 Å) using eq 6 with the indicated distances estimated from structural studies (Figure 5B).

When S1 was bound to actin, the transferred lifetime increased about 10% (Table 1), indicating that the average distance between Tm molecules increased. From the lifetime change, it is calculated that the energy-transfer efficiency decreased from 28 to 21.0%, which corresponds to an apparent distance increase from 67 to 71 Å.

We also monitored the effect of Tn and Ca^{2+} on the energy transfer. Tn decreased the donor-alone lifetime from 1.43 to 1.25 ms, independent of Ca^{2+}, indicating a direct interaction between Tn and Tm in the region of the donor at Cys 190 (Table 1) as indicated earlier (*55*). The energy-transfer efficiency and the distance calculated from the data in the presence of the acceptor showed that Tn ± Ca^{2+} did not change the Tm−Tm energy transfer across the actin filament. However, as in the case of actin−Tm, for actin−Tm−Tn ± Ca^{2+}, addition of S1 increased the apparent Tm−Tm distance about 5 Å.

To determine that the component with the unchanged lifetime was not due to unbound Tm or Tb chelate, the samples were measured again after centrifuging to a pellet the reconstituted thin filaments, homogenizing the pellets in sample buffer, and repeating the lifetime measurements. The results were similar to the original results.

DISCUSSION

Advantages of NbS·SCy-DTPA-Cs124. In this paper, we synthesized NbS·SCy-DTPA-Cs124 and used its Tb^{3+} chelate as a donor and rhodamine maleimide as an acceptor in energy-transfer experiments between Cys sites on Tm. This class of Tb^{3+} probes originally developed by Selvin and coworkers to be used as donors in LRET measurements has been reviewed (*44*) and used in several applications (*22*−*25*). Chelated Tb^{3+} exhibits luminescence with a lifetime in the millisecond range, and Cs124, the antenna moiety used here, has appreciable absorption at 337 nm and can therefore be excited with a low power N_2 laser. Its emission is efficiently transferred to Tb^{3+} in the chelate. Lifetimes in the millisecond range allow for direct acquisition and gating methods to obtain the decay profile. The high quantum yield of the Tb^{3+} chelate and the good overlap of its emission with the rhodamine absorption band allow large distances to ∼80 Å to be determined. The narrow emission bands of Tb^{3+} facilitate both the direct observation of the total Tb^{3+} decay and the rhodamine-detected Tb^{3+} emission transfer. Thus, it is possible to monitor only the transferred millisecond Tb^{3+} (indirect) emission in the rhodamine band, where Tb^{3+} does not directly emit, by gating out the nanosecond rhodamine fluorescence. However, the ringing of the PMT because of the intense rhodamine fluorescence could not be completely gated out in this paper. Other methods have been used to attempt to solve this problem (*40*). Distances can also be more accurately obtained because the Tb^{3+} emission is unpolarized, allowing for the use of the random $^2/_3$ value for the orientation parameter, k^2, in the calculation of R_0.

Our probe is particularly useful as a labeling reagent for Cys groups because the NbS group reacts efficiently and only with Cys in a manner similar to the previously used 2-pyridyl

Table 1: Tm^D-Tm^A Distances Across the Actin Filament in the Absence and Presence of Tn, Ca^{2+}, and S1[a]

sample	donor lifetime λ_D (ms)	λ (nm)	donor−acceptor lifetimes (ms)	ET (%)	distance R (Å)
Tm + F actin	1.44	545	0.30 (0.10), **1.01** (0.44), 1.44 (0.46)	27.8	66.8
		568	0.04 (0.56), 0.26 (0.16), **1.04** (0.28)	±2	±1.2
Tm + F actin + S1	1.44	545	0.35 (0.09), **1.13** (0.42), 1.43 (0.49)	21.5	70.7
		568	0.03 (0.51), 0.29 (0.18), **1.13** (0.31)	±3	±1.8
Tm + F actin + Tn ($-Ca^{2+}$)	1.26	545	0.28 (0.27), **0.97** (0.36), 1.26 (0.37)	26.2	67.7
		568	0.03 (0.57), 0.24 (0.19), **0.93** (0.24)	±3	±2.0
Tm + F actin + Tn ($+Ca^{2+}$)	1.24	545	0.28 (0.26), **0.92** (0.37), 1.24 (0.37)	27.4	67.0
		568	0.02 (0.63), 0.19 (0.15), **0.90** (0.22)	±1.6	±1.0
Tm + F actin + Tn + S1 ($-Ca^{2+}$)	1.26	545	0.33 (0.27), **1.04** (0.33), 1.26 (0.40)	19.8	71.9
		568	0.03 (0.67), 0.26 (0.14), **1.01** (0.19)	±2.4	±1.9
Tm + F actin + Tn + S1 ($+Ca^{2+}$)	1.24	545	0.34 (0.28), **1.02** (0.24), 1.24 (0.48)	19.4	72.3
		568	0.02 (0.67), 0.26 (0.14), **1.00** (0.19)	±1.7	±1.3

[a] Donor−acceptor decays were fit to 3 lifetimes, and the bold lifetime, τ_{DA}, was used to calculated the efficiency of energy transfer.

group (*21*) to liberate absorbing species, which can quantitatively monitor the labeling reaction. However, the NbS group has an advantage over the 2-pyridyl group in that its liberated NbS ion absorbs at 412 nm, which does not overlap with the Cs124 antenna absorbance, allowing more accurate labeling information to be obtained. A property of the disulfide-containing labels compared to the maleimide that one must be aware of is that the disulfide label can be removed on exposure to high concentrations of SH reagents such as DTT.

LRET Distance within Tm. For a control experiment, we compared the LRET-determined average distance between Cys 56 on one chain and Cys 100 on the other chain of the in-register heterodimeric-labeled mutant Tm with the known distance obtained from an equivalent position of the coordinates of the crystal structure of an 80-residue Tm coiled-coil peptide (*41*). The smaller value in solution (55 Å) compared with that calculated from structural data (65 Å) is consistent with the probe motion because of the flexibility of Tm in solution. We also checked the distance changes at different temperatures. The apparent distance changed from 55 to 53 Å (energy transfer from 50 to 60%) when the temperature was increased from 10 to 50 °C. The decrease in apparent distance suggests an increase in flexibility with temperature.

This smaller average distance is a consequence of the millisecond donor lifetime because microsecond motion of the probe will bring the donor closer to the acceptor resulting in a closer average distance, increasing the probability of energy transfer. The small decrease in the average distance on binding to actin is consistent with some immobilization on actin. Similar conclusions were reached with phosphorescence anisotropy studies (*45*). In a different system, a shorter distance between a similar millisecond Tb^{3+} millisecond probe compared to a nanosecond Cy5 probe transferring to rhodamine−maleimide was explained by probe dynamics (*46*); i.e., microsecond motion would allow for more transfer during the millisecond lifetime but not during the nanosecond lifetime. Independent probe motion about single C−C bonds may occur, but it is expected to be of a relatively small amplitude so as to not appreciably affect the transfer rate. It is difficult to know the precise submillisecond motion that contributes to the flexibility, but EM images of individual Tm molecules show that they are not rigid (*47*). Also, hydrodynamic measurements of coiled coils indicated that they were semiflexible ropelike molecules with a persistence length of 1300 Å (*48*). Thus, regions could bend 5−10 Å in a distance of one or two molecular lengths of 400−800 Å (*49*).

Energy Transfer between Tm's on the Actin Thin Filament. Energy transfer from Tm molecules with donor-labeled Cys surrounded by acceptor-labeled Tm molecules could only take place across the actin filament because equivalent cystines along the long pitch thin filament are too far apart (∼400 Å).

Many early structural studies showed that Tm binds to actin at a radius of about 38−40 Å from the filament axis (*27*−*30*). Thus, the distance between the Tm filaments across the actin is about 76−80 Å. The distance between equivalent α carbons of Cys 190 ranges from 76 Å for the closest chains to 84 Å for the furthest chains (*30*), which changes somewhat with a reasonable estimate of the location of the probes on the α carbons (*17*) (Figure 5B). An apparent distance, r_a, can be calculated from eq 6 for each of the donors to both acceptors. The average apparent distance obtained was 73 Å. The LRET-determined distance for actin−Tm in the absence and presence of Tn determined in this paper is about 67 Å. The significantly shorter distance between Tm's across the actin filament than expected appears to be due to the movement of Tm on actin in the submillisecond range. Flexing and/or torsional motions of Tm on the surface of F actin in the microsecond range would bring the donor and acceptor probes closer during the millisecond lifetime of the donor, as discussed above. Tm flexibility has been suggested from structural studies (*30*), from modeling studies (*50*, *51*), and spectroscopic studies (*43*, *45*, *52*). This flexibility may play an important role in regulation.

For actin−Tm−Tn-reconstituted thin filaments, the LRET data indicated that Ca^{2+} did not produce a significant change in the Tm−Tm intermolecular distance. Previous EM studies indicated that Tm moved about 25° on the surface of actin induced by Ca^{2+} (*8*−*11*). Our earlier study using FRET measurements showed that the data were consistent with a 17° rolling of Tm over the actin surface (*17*). However, the movement did not change the radial distance between Tm axes. The resolution of the LRET measurements made here were not as high as the FRET measurements, allowing only a single average apparent distance from the two donors to be obtained. Therefore, the lack of change of the apparent Tm−Tm distance is consistent with a lack of change of the radial distance of the Tm axis from the actin axis. The lack of an effect of Ca^{2+} also suggests little or no change in flexibility because of Ca^{2+} binding to troponin in the thin filament (see below).

For actin−Tm−Tn and actin−Tm, addition of saturating S1 caused a small but significant increase in the apparent distance between Tm's. This can either be due to an actual increase in the average distance or a decrease in flexibility. As discussed above, the Tm−Tm distance obtained by LRET in the absence of S1 is appreciably smaller than what has been determined from structural studies, probably because of the effects of motion of Tm. The 4−5-Å larger apparent distance produced by S1 binding to actin suggests some immobilization of Tm on actin because of S1 binding to actin, which would decrease the motion leading to a greater apparent distance; i.e., the sampling of the closer distances associated with the motion would decrease. This result is consistent with the polarized phosphorescence studies on the erythrosine-labeled Tm (*45*). The measured anisotropy of the skeletal Tm−actin complex changed from 0.025 to 0.049 when S1 was added, indicating that myosin binding significantly blocks the microsecond rotational motions of Tm on the surface of actin (*45*).

Stoichiometric S1 binding in the absence of ATP (rigor complexes) to actin−Tm and actin−Tm−Tn, even in the absence of Ca^{2+}, induces Tm to move to the open state (*1*). Thus, it is not surprising that a similar change in transfer occurred for those systems.

Both structural and FRET studies provided evidence for Tm movement induced by the myosin head binding to actin. Three dimensional electron microscopic reconstruction observed a 10° azimuthal Tm movement around actin induced by the myosin heads binding in addition to the movement induced by Ca^{2+} (*9*). This is consistent with the three regulatory states of the thin filament (*6*). FRET studies of S1-induced movement of gizzard-muscle Tm obtained a S1-induced Tm movement of ∼6−8 Å between Tm and actin, consistent with a rolling motion at a constant radius (*20*).

Are Tm Molecules In-Register on Actin? There is considerable evidence that 1 Tm binds to 7 actin subunits, leaving few if any gaps between neighboring Tm's (*53*, *54*), in agreement with the relatively strong end−end interactions that occur, particularly in the presence of Tn (*55*). However, the possibility exists that for reconstituted filaments, particularly in the absence of Tn, there are different numbers of bare actin subunits at the filament ends as well as some gaps in the middle, which could lead to Tm's across the actin filament not being in-register. The presence of excess actin in these experiments may also contribute to the presence of gaps. For random binding, energy transfer would only take place for 2 of 7 relative binding modes where neighboring Tm's are within transfer distance. If a fraction of the Tm's do not see acceptors, the amplitude of the transferred component (the shortened lifetime) would be decreased from 1.0. The observation that there was incomplete transfer (Table 1) suggests the possibility of some nonregistered binding of Tm's. Of course, incomplete transfer could be due to unbound Tm and a contribution of donor-labeled Tm's adjacent to each other. However, we noted above that resuspension of pelleted filaments gave the same result. Also, assuming random neighbor formation on renaturation, with a 4:1 ratio of acceptor/donor, only a small fraction of donor-labeled molecules would be neighbors and would not contribute to the transfer.

To check the possibility of Tm's out of register across the filament, we measured the distances between mutant gizzard-muscle Tm mixtures containing labels at different Cys positions. These labeled mutants allowed for potential transfer from positions 56−56, 56−190, 100−100, and 100−190 as well as the previously discussed positions 190−190. All of the LRET measurements gave similar distances between the different sites across actin, 64−67 Å (Table 2). If Tm molecules are in-register across the actin filament, the distance between these nonequivalent sites would be too far for energy transfer to take place; e.g., 200 Å separates position 56 and 190. These data suggest the existence of some out of register Tm binding in these reconstituted filaments (*54*). Previous data with native thin filaments or filaments containing Tn indicated that the Tm's were in-register (*55*, *56*). It is possible that some random binding takes place in solution, especially in the absence of Tn when end−end interactions are weaker. There is also the possibility of thin-filament aggregation bringing Tm's close together.

Table 2: Tm^D−Tm^A Distances Across the Actin Filament between Probes at Two Different Sites on Tm

donor	acceptor	τ_D (ms)	τ_{DA} (ms)	ET (%)	distance (Å)
Tm56	Tm56	1.20	0.81	32.5	64.4
Tm56	Tm190	1.20	0.84	30.0	65.6
Tm100	Tm100	1.12	0.79	29.5	66.0
Tm100	Tm190	1.12	0.77	31.3	65.0
Tm190	Tm190	1.44	1.04	27.8	66.8

In conclusion, (1) a new Cys-directed Tb^{3+} label useful for LRET measurements has been synthesized; (2) labeled Tm bound to actin shows fluorescence energy transfer across the actin filament; (3) in the reconstituted actin−Tm−Tn thin filament, Ca^{2+} did not change the distance; (4) S1 produced a 4-Å increase in the apparent distance; and (5) distances obtained with this millisecond probe appear shorter than expected, suggesting Tm flexibility.

ACKNOWLEDGMENT

We thank Dr. Corrado Bacchiocchi for some of the inter-Tm distance calculations and Ms. Tanya Freedman and Ms. Rebecca Stewart for help in protein preparation.

REFERENCES

1. Lehrer, S. S., and Geeves M. A. (1998) The muscle thin filament as a classical cooperative/allosteric regulatory system, *J. Mol. Biol. 277*, 1091−1089.
2. Perry, S. V. (2001) Vertebrate tropomyosin: Distribution, properties, and function, *J. Musc. Res. Cell Motil. 22*, 5−49.
3. Huxley, H. E. (1972) Structural changes in actin- and myosin-containing filaments during contraction, *Cold Spring Harbor Symp. Quantum Biol. 37*, 361−376.
4. Haselgrove, J. C. (1972) X-ray evidence for a conformational change in the actin-containing filaments of vertebrate striated muscle, *Cold Spring Harbor Symp. Quantum Biol. 37*, 341−352.
5. Parry, D. A. D., and Squire, J. M. (1973). Structural role of tropomyosin in muscle regulation: Analysis of the X-ray diffraction patterns from relaxed and contracting muscles, *J. Mol. Biol. 75*, 33−55.
6. Mckillop, D. F. A., and Geeves, M. A. (1993) Regulation of the interaction between actin and myosin subfragment 1: Evidence of three states of the thin filament, *Biophys. J. 65*, 693−701.
7. Lehman, W., Craig, R., and Vibert, P. (1994) Ca^{2+}-induced tropomyosin movement in Limulus thin filaments revealed by three-dimensional reconstruction, *Nature 368*, 65−67.
8. Vibert, P., Craig, R., and Lehman, W. (1997) Steric-model for activation of muscle thin filaments, *J. Mol. Biol. 266*, 8−14.

9. Xu, C., Craig, R., Tobacman, L., Horowitz, R., and Lehman, W. (1999) Tropomyosin positions in regulated thin filaments revealed by cryoelectron microscopy, *Biophys. J. 77*, 985−992.
10. Craig, R., and Lehman, W. (2001) Crossbridge and tropomyosin positions observed in native, interacting thick and thin filaments, *J. Mol. Biol. 311*, 1027−1036.
11. Narita, A., Yasunaga, T., Ishikawa, T., Mayanagi, K., and Wakabayashi, T. (2001) Ca^{2+}-induced switching of troponin and tropomyosin on actin filaments as revealed by electron cryo-microscopy, *J. Mol. Biol. 308*, 241−261.
12. Tao, T., Lamkin, M., and Lehrer, S. S. (1983) Excitation energy transfer studies of the proximity between tropomyosin and actin in reconstituted skeletal muscle thin filaments, *Biochemistry 22*, 3059−3066.
13. Miki, M., Miura, T., Sano, K., Kimura, H., Kondo, H., Ishida, H., and Maeda, Y. (1998) Fluorescence resonance energy transfer between points on tropomyosin and actin in skeletal muscle thin filaments: Does tropomyosin move? *J. Biochem. 123*, 1104−1111.
14. Hai, H., Sano, K., Maeda, K., Maeda, Y., and Miki, M. (2002) Ca^{2+}- and S1-induced conformational changes of reconstituted skeletal muscle thin filaments observed by fluorescence energy transfer spectroscopy: Structural evidence for three states of thin filament, *J. Biochem. 131*, 407−418.
15. Tao, T., Gong, B. J., and Leavis, P. C. (1990) Calcium-induced movement of troponin-I relative to actin in skeletal muscle thin filaments, *Science 247*, 1339−1341.
16. Miki, M., Kobayashi, T., Kimura, H., Hagiwara, A., Hai, H., and Maeda, Y. (1998) Ca^{2+}-induced distance change between points on actin and troponin in skeletal muscle thin filaments estimated by fluorescence energy transfer spectroscopy, *J. Biochem. 123*, 324−331.
17. Bacchiocchi, C., and Lehrer, S. S. (2002) Ca^{2+}-induced movement of tropomyosin in skeletal muscle thin filaments observed by multi-site FRET, *Biophys. J. 82*, 1524−1536.
18. Graceffa, P. (1999) Movement of smooth muscle tropomyosin by myosin heads, *Biochemistry 38*, 11984−11992.
19. Graceffa, P. (2000) Phosphorylation of smooth muscle myosin heads regulates the head-induced movement of tropomyosin, *J. Biol. Chem. 275*, 17143−17148.
20. Bacchiocchi, C., Graceffa, P., and Lehrer, S. S. (2004) Myosin-induced movement of $\alpha\alpha$, $\alpha\beta$, and $\beta\beta$ smooth muscle tropomyosin on actin observed by multisite FRET, *Biophys. J. 86*, 2295−2307.
21. Chen, J. Y., and Selvin, P. R. (1999) Thiol-reactive luminescent chelates of terbium and europium, *Bioconjugate Chem. 10*, 311−315.
22. Getz, E. B., Cooke, R., and Selvin, P. R. (1998) Luminescence resonance energy transfer measurements in myosin, *Biophys. J. 74*, 2451−2458.
23. Cha, A., Snyder, G. E., Selvin, P. R., and Bezanilla, F. (1999) Atomic scale movement of the voltage-sensing region in a potassium channel measured via spectroscopy, *Nature 402*, 809−813.
24. Xiao, M., Li, H., Snyder, G. E., Cooke, R., Yount, R. G., and Selvin, P. R. (1998) Conformational changes between the active-site and regulatory light chain of myosin as determined by luminescence resonance energy transfer: The effect of nucleotides and actin, *Proc. Natl. Acad. Sci. U.S.A. 95*, 15309−15314.
25. Chakrabarty, T., Xiao, M., Cooke, R., and Selvin, P. R. (2002) Holding two heads together: Stability of the myosin II rod measured by resonance energy transfer between the heads, *Proc. Natl. Acad. Sci. U.S.A. 99*, 6011−6016.
26. Root, D. D. (1997) In situ molecular association of dystrophin with actin revealed by sensitized emission immuno-resonance energy transfer, *Proc. Natl. Acad. Sci. U.S.A. 94*, 5685−5690.
27. Vazquez-lbar, J. L., Weinglass, A. B., and Kaback, H. R. (2001) Engineering a terbium-binding site into an integral membrane protein for luminescence energy transfer, *Proc. Natl. Acad. Sci. U.S.A. 99*, 3487−3492.
28. Bertrand, R., Derancourt, J., and Kassab, R. (2000) Fluorescence characterization of structural transitions at the strong actin binding motif in skeletal myosin affinity labeled at cysteine 540 with novel spectroscopic cysteaminyl mixed disulfides, *Biochemistry 39*, 14626−14637.
29. Bertrand, R., Capony, J. P., Derancourt, J., and Kassab, R. (1999) Detection of nucleotide- and F-actin-induced movements in the switch II helix of the skeletal myosin using its differential oxidative cleavage mediated by and iron−EDTA complex disulfide-linked to the strong actin binding site, *Biochemistry 38*, 11914−11925.
30. Lorenz, M., Poole, K. J. V., Popp, D., Rosenbaum, G., and Holmes, K. C. (1995) An atomic model of the unregulated thin filament obtained by X-ray fiber diffraction on oriented actin−tropomyosin gels, *J. Mol. Biol. 246*, 108−119.
31. Milligan, R. A., and Flicker, P. F. (1987) Structural relationships of actin, myosin, and tropomyosin revealed by cryo-electron microscopy, *J. Cell Biol. 105*, 29−39.
32. Milligan, R. A., Whittaker, M., and Safer, D. (1990) Molecular structure of F-actin and location of surface binding sites, *Nature, 348*, 217−221.
33. Bivin, D. B., Stone, D. B., Schneider, D. K., and Mendelson R. A. (1991) Cross-helix separation of tropomyosin molecules in acto-tropomyosin as determined by neutron scattering, *Biophys. J. 59*, 880−888.
34. Golitsina, N. L., and Lehrer, S. S. (1999) Smooth muscle α-tropomyosin crosslinks to caldesmon, to actin and to myosin subfragment 1 on the muscle thin filament, *FEBS Lett. 463*, 146−150.
35. Ajtai, K., Ilich, P. J. K., Ringler, A., Sedarous, S. S., Toft, D. J., and Burghardt, T. J. (1992) Stereospecific reaction of muscle fiber proteins with the 5′ or 6′ isomer of (iodoacetamido)tetramethyl-rhodamine, *Biochemistry 31*, 12431−12440.
36. Hamman, B. D., Oleinikov, A. V., Jokhadze, G. G., Bochkariov, D. E., Traut, R. R., Jameson, D. M. (1996) Tetramethylrhodamine dimer formation as a spectroscopic probe of the conformation of *Escherichia coli* ribosomal protein L7/L12 dimers, *J. Biol. Chem. 271*, 7568−7573.
37. Lakowicz, J. R. (1999) *Principles of Fluorescence Spectroscopy*, 2nd ed., Kluwer Academic/Plenum Publishers, New York.
38. Xiao, M., and Selvin, P. R. (2001) Quantum yields of luminescent lanthanide chelates and far-red dyes measured by resonance energy transfer, *J. Am. Chem. Soc. 123*, 7067−7073.
39. Lehrer, S. S. (1975) Intramolecular crosslinking of tropomyosin via disulfide bond formation: Evidence for chain register, *Proc. Natl. Acad. Sci. U.S.A. 72*, 3377−3381.
40. Xiao, M., and Selvin, P. R. (1999) An improved instrument for measuring time-resolved lanthanide emission and resonance energy transfer, *Rev. Sci. Instrum. 70*, 3877−3881.
41. Brown, J. H., Kim, K. H., Jun, G., Greenfield, N. J., Dominguez, R., Volkmann, N., Hitchcock-DeGregori, S. E., and Cohen, C. (2001) Deciphering the design of the tropomyosin molecule, *Proc. Natl. Acad. Sci. U.S.A. 98*, 8496−8501.
42. Ishii, Y., and Lehrer, S. S. (1987) Fluorescence probe studies of the state of tropomyosin in reconstituted muscle thin filaments, *Biochemistry 26*, 4922−4925.
43. Szczesna, D., and Fajer, P. G. (1995) The tropomyosin domain is flexible and disordered in reconstituted thin filaments, *Biochemistry 34*, 3614−3620.
44. Selvin, P. R., and Hearst, J. E. (1994) Luminescence energy transfer using a terbium chelate: Improvements on fluorescence energy transfer, *Proc. Natl. Acad. Sci. U.S.A. 91*, 10024−10028.
45. Chandy, I. K., Lo, J. C., and Ludescher, R. D. (1999) Differential mobility of skeletal and cardiac tropomyosin on the surface of F-actin, *Biochemistry 38*, 9286−9294.
46. Xiao, M., Reifenberger, J. G., Wells, A. L., Baldacchino, C., Chen, L. Q., Ge, P., Sweeney, H. L., and Selvin, P. R. (2003) An actin-dependent conformational change in myosin, *Nat. Struct. Biol. 10*, 402−408.
47. Flicker, P. F., Phillips, G. N., Jr., Cohen, C. (1982) Troponin and its interactions with tropomyosin. An electron microscope study, *J. Mol. Biol. 162*, 495−501.
48. Hvidt, S., Ferry, J. D., Reolke, D. L., and Greaser, J. L. (1983) Flexibility of light meromyosin and other coiled-coil α-helical proteins, *Macromolecules 16*, 740−745.
49. Lehrer, S. S., Golitsina, N., and Geeves, M. A. (1997) Actin−tropomyosin activation of myosin subfragment 1 ATPase and thin filament cooperativity. The role of tropomyosin flexibility and end-to-end interactions, *Biochemistry 36*, 13449−13454.
50. Smith, D. A., and Geeves, M. A. (2003) Cooperative regulation of myosin−actin interactions by a continuous flexible chain II: Actin−tropomyosin−troponin and regulation by calcium, *Biophys. J. 84*, 3168−3180.
51. Smith, D. A., Maytum, R., and Geeves, M. A. (2003) Cooperative regulation of myosin−actin interactions by a continuous flexible chain I: Actin−tropomyosin systems, *Biophys. J. 84*, 3155−3167.

52. Ishii, Y., and Lehrer, S. S. (1990) Excimer fluorescence of pyrenyliodoacetamide-labeled tropomyosin: A probe of the state of tropomyosin in reconstituted muscle thin filaments, *Biochemistry 29*, 1160−1166.
53. Wegner, A. (1979) Equilibrium of the actin−tropomyosin interaction, *J. Mol. Biol. 131*, 839−853.
54. Vilfan, A. (2001) The binding dynamics of tropomyosin on actin, *Biophys. J. 81*, 3146−3155.
55. Wray, J., Vibert, P., and Cohen, C. (1978) Actin filaments in muscle: Pattern of myosin and tropomyosin/troponin attachments, *J. Mol. Biol. 124*, 501−521.
56. Ohtsuki, I. (1979) Molecular arrangement of troponin-T in the thin filament, *J. Biochem. 86*, 491−497.

BI049186V